# Electronic susceptibilities in systems with anisotropic Fermi surfaces

S. Fratini* and F. Guinea
*Instituto de Ciencia de Materiales de Madrid, CSIC, Cantoblanco, E-28049 Madrid, Spain*
(Received 22 April 2002; published 23 September 2002)

The low-temperature dependence of the spin and charge susceptibilities of an anisotropic electron system in two dimensions is analyzed. It is shown that the presence of inflection points at the Fermi surface leads, generically, to a $T \ln T$ dependence, and a more singular behavior, $\chi \sim T^{3/4} \ln T$, is also possible. Applications to quasi-two-dimensional materials are discussed.

DOI: 10.1103/PhysRevB.66.125104 PACS number(s): 71.10.Ay, 74.20.Mn, 71.10.Pm, 05.30.Fk

## I. INTRODUCTION

The possible existence of quantum critical points in the phase diagrams of many materials has led to a detailed study of the low-temperature behavior of the susceptibilities of electron systems. The critical properties of the system are determined by the energy and momentum dependence of the response function of the electron system associated with the order parameter in the ordered phase.[1–3] It has been shown that the low-temperature spin susceptibility of the isotropic electron liquid has an unexpected nonanalytic dependence on temperature, when high-order perturbative corrections are considered.[4] These corrections are irrelevant in the renormalization group sense,[5–7] and do not modify the basic properties of the electron liquid, as described by Landau's theory. However, they can lead to unexpected power-law dependences in many physical quantities at low temperatures, or change the order of the phase transitions.[8] The origin of these nonanalyticities in homogeneous response functions has been traced back to the special properties of $2k_F$ scattering in the isotropic electron liquid.[9]

It is well known that anisotropic Fermi surfaces can have regions where scattering becomes more singular than in the isotropic electron liquid, the so-called hot spots. When two portions of the Fermi surface are flat and parallel, nesting occurs, and the susceptibilities diverge logarithmically, $\mathrm{Re}\,\chi(\vec{\mathbf{Q}},\omega) \propto \log(\Lambda/\omega)$, where $\vec{\mathbf{Q}}$ is the nesting vector. A saddle point in the density of states leads also to logarithmic divergences in two dimensions. The hot spots at the Fermi surface can be characterized by the frequency dependence of $\mathrm{Im}\chi(\vec{\mathbf{Q}},\omega)$, where $\vec{\mathbf{Q}}$ spans the hot spots. The usual behavior in a Fermi liquid is $\mathrm{Im}\,\chi(\vec{\mathbf{Q}},\omega) \propto |\omega|$ in any dimension $D$. For an isotropic Fermi surface, if $|\vec{\mathbf{Q}}| = 2k_F$, one has $\mathrm{Im}\,\chi(\vec{\mathbf{Q}},\omega) \propto |\omega|^{(D-1)/2}$. For $D=1$ the imaginary part of the $2k_F$ susceptibility approaches a constant at low frequencies. By a Kramers-Kronig transformation, it can be shown that the real part should diverge logarithmically, leading to the deviations from Landau's theory which characterize a Luttinger liquid.

It is also possible to show that, when $\vec{\mathbf{Q}}$ connects two saddle points in an anisotropic Fermi surface (FS), $\mathrm{Im}\,\chi(\vec{\mathbf{Q}},\omega) \propto |\omega|^{(D-2)/2}$. This result implies the existence of logarithmic divergences for $D=2$, which have been extensively studied in relation to high-$T_c$ superconductors,[10] and lead to deviations from Landau's theory.[11] In addition to saddle points, a generic anisotropic Fermi surface can show inflection points (see Fig. 1). The existence of these points at the Fermi surface, which do not require any special fine tuning of the chemical potential, leads to[12] $\mathrm{Im}\,\chi(\vec{\mathbf{Q}},\omega) \propto |\omega|^{(D-2)/2+1/4}$. For $D=2$, scattering between these points is more singular than the $2k_F$ scattering considered previously, but still not sufficient to invalidate the Fermi-liquid theory.[10,13]

In the present work, we analyze scattering at inflection points in a two-dimensional anisotropic Fermi surface. In the following section, we present the main features of the second-order perturbative calculation, extending the method used in Ref. 9. The main results are obtained in Sec. III, while the finer details of the calculation are deferred to the Appendixes. Applications to Fermi surfaces of different shapes are given in Sec. IV, and Sec. V discusses the main results of our work.

## II. THE METHOD

We consider a system of two-dimensional (2D) fermions interacting through a generic isotropic short-ranged effective potential $U(q)$, assuming that long-range interactions are screened. For the sake of simplicity, we shall also assume that the interaction only affects electrons of opposite spins, which is a reasonable approximation when the momentum dependence of $U(q)$ is weak. It was shown in Refs. 4 and 9 that while the lowest-order ($\propto U$) perturbative corrections are well behaved, higher-order corrections can lead to an anomalous behavior in the low-energy properties of the Fermi liquid. To be more precise, the uniform spin suscepti-

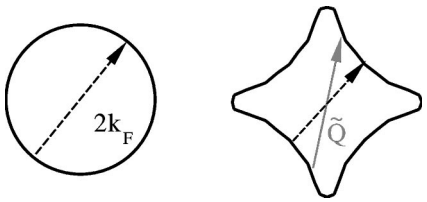


FIG. 1. Examples of Fermi surfaces in two spatial dimensions. Left: circular, all wave vectors of modulus $2k_F$ are sources of enhanced scattering. Right: anisotropic, wave vectors such as $\tilde{\mathbf{Q}}$ connecting two inflection points give rise to anomalous scattering (continuous arrow), while the rest of the FS gives rise to a behavior similar to the isotropic case (dashed arrow).

 

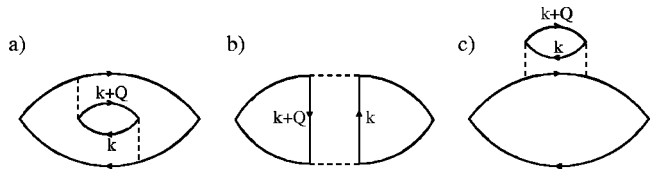


FIG. 2. The second-order diagrams yielding the leading temperature dependence of the susceptibility.

bility of a 2D electron system shows a linear $T$ dependence, which contradicts the usual Sommerfeld expansion in powers of $(T/E_F)^2$. Such anomalous behavior was traced back to the peculiarities of $2k_F$ scattering, i.e., the occurrence of particle-hole pairs lying on opposite sides of the FS. This special wave vector plays a key role in the $q$-dependent susceptibility of electronic systems already in the noninteracting case, with the appearance of a square-root singularity around $2k_F$, which is directly related to the jump in the occupation number. If one considers the *uniform* susceptibility, though, the singularities associated with $2k_F$ scattering can only show up indirectly through the excitation of a *virtual* particle-hole pair, which explains the absence of anomalous corrections at lowest order in the interaction strength.

In the general (noncircular) case, among all the wave vectors connecting opposite sides of the FS, the inflection points play a special role due to the flatness of the Fermi surface (the extreme case being that of a perfectly flat FS, or perfect nesting, which leads to strong instabilities). According to the previous discussion, the second-order diagrams which lead to nonstandard behavior are those containing a particle-hole bubble whose transferred momentum can match the special value $\tilde{\mathbf{Q}}$. Such diagrams are depicted in Fig. 2. Diagrams (a) and (b) are vertex corrections. They have opposite signs and cancel in the case of a perfectly $q$-independent interaction potential: the fermion propagators involved are the same in both diagrams, the only difference being in the momentum carried by the interaction. To be specific, with the notations of Fig. 2, diagram (a) is proportional to $U(\tilde{\mathbf{Q}})^2$, while diagram (b) involves some momentum average of the interaction, and there is no reason for a perfect cancellation in the general case. Diagram (c) is a self-energy correction, and will be considered separately.

## III. UNIFORM SUSCEPTIBILITIES

After integration over Matsubara frequencies, the vertex correction (a) of Fig. 2 in the zero-frequency, zero-momentum limit reads

$$\chi(T)=\int \frac{d^2p}{(2\pi)^2}\frac{d^2Q}{(2\pi)^2}U(\mathbf{Q})^2\Delta(\xi_{\mathbf{p}}) \times\Delta(\xi_{\mathbf{p}+\mathbf{Q}})L(\xi_{\mathbf{p}+\mathbf{Q}}-\xi_{\mathbf{p}},\mathbf{Q}), \tag{1}$$

where the Lindhard function in two space dimensions is defined as

$$L(i\Omega,Q)=\int \frac{d^2k}{(2\pi)^2}\frac{n(\xi_{\mathbf{k}})-n(\xi_{\mathbf{k}+\mathbf{Q}})}{i\Omega+\xi_{\mathbf{k}}-\xi_{\mathbf{k}+\mathbf{Q}}} \tag{2}$$

and[14] $\Delta(\xi)=\beta/4\cosh^2(\beta\xi/2)$. Such $\Delta$ functions, which constrain momenta to lie within a shell of thickness $\sim T$ from the Fermi surface, are strongly temperature dependent, and are responsible for the leading temperature dependence of the susceptibility. Indeed, in Eq. (1) we have omitted terms proportional to $\Delta(\xi_{\mathbf{p}+\mathbf{Q}})n(\xi_{\mathbf{p}})$ coming from the poles of the Lindhard function, which are less $T$ dependent since they receive contributions mainly from regions far from the Fermi surface. Taking advantage of time-reversal symmetry ($\xi_{\mathbf{k}}=\xi_{-\mathbf{k}}$), we can write

$$L(\Delta\xi_p,Q)=\int \frac{d^2k}{(2\pi)^2}n(\xi_{\mathbf{k}})\left[\frac{1}{\Delta\xi_{\mathbf{p}}-\Delta\xi_{\mathbf{k}}}-\frac{1}{\Delta\xi_{\mathbf{p}}+\Delta\xi_{\mathbf{k}}}\right], \tag{3}$$

where we have defined $\Delta\xi_{\mathbf{k}}=\xi_{\mathbf{k}+\mathbf{Q}}-\xi_{\mathbf{k}}$. As was pointed out in the preceding section, the most singular contributions to Eq. (1) come from regions where the momentum $\mathbf{Q}$ flowing through the Lindhard function $L$ connects parts of the FS which are almost parallel, since this makes the denominators in Eq. (3) small on large regions of $k$ space. Otherwise stated, the scattering processes taking place within a particle-hole pair are enhanced around special wave vectors $\tilde{\mathbf{Q}}$ due to the peculiar geometry of the FS. In the case of a spherically symmetric FS, any momentum $\tilde{\mathbf{Q}}$ of modulus $2k_F$ is a source of enhanced scattering, but the deviation from parallelism is *quadratic* as we move in the direction tangent to the surface (see Fig. 1, left). More singular is the case of inflection points occurring when the curvature of the FS vanishes, leading to a *cubic*, or even *quartic* dispersion (see Fig. 1, right), which is a quite generic phenomenon when dealing with electrons on a lattice.

In the following sections, we shall present the calculation of the leading $T$ dependence of the diagram (a) in the simplest circular case as well as for more complex FS shapes. The result for diagram (b) can obtained by replacing $U(\mathbf{Q})$ by $U(\mathbf{p}-\mathbf{k})$ in Eq. (1). This can only lead to a change in the prefactors, but will not alter the leading temperature dependence of the susceptibility. The self-energy diagram (c) has a different structure, and will be analyzed at the end of the section.

### A. Isotropic Fermi surface

By choosing an appropriate coordinate system, the dispersion relation around any point on a spherical FS (and, generically, about nonspecial points of an anisotropic FS) can be expanded as

$$\xi_{\mathbf{k}}/v=k_y+ak_x^2, \tag{4}$$

$v$ being the Fermi velocity at that particular point (that we shall identify as $\tilde{\mathbf{Q}}/2$), and $a>0$ being related to the FS curvature. The above expression is assumed to be valid up to a momentum cutoff $\Lambda$ which is larger than that imposed by the finite temperature $\Delta$ functions.[15] Introducing $\mathbf{q}=\mathbf{Q}-\tilde{\mathbf{Q}}$, we can write

$$\xi_{\mathbf{k}+\mathbf{Q}}/v=-(k_y+q_y)+a(k_x+q_x)^2, \tag{5}$$

where we have used the property $\xi_{\mathbf{k}+\tilde{\mathbf{Q}}}=\xi_{-\mathbf{k}}$ (reflection symmetry). We now change variables to

$$k_\perp = k_y + a k_x^2, \tag{6}$$

$$k_\parallel = k_x + q_x/2,$$

such that $\xi_{\mathbf{k}}=v k_\perp$ and

$$\xi_{\mathbf{k}+\mathbf{Q}}/v = -k_\perp - q_\perp + 2a k_\parallel^2 + (3/2) a q_\parallel^2 . \tag{7}$$

Apart from the constant shift $q_x/2$ introduced for later convenience, this new coordinate system is locally equivalent to polar coordinates, which would be the natural choice when dealing with a perfectly symmetric FS. We shall focus on the first term in Eq. (3), which is independent of $q_\perp$, and therefore turns out to be the most singular. Omitting unimportant multiplicative factors, we have for the real part of $L$,

$$L = \frac{-1}{v}\int dk_\perp n(v k_\perp) \int_{-\Lambda}^{\Lambda} dk_\parallel \frac{1}{A - 2k_\perp + B k_\parallel^2}$$

$$= \frac{-1}{v\sqrt{B}}\int dk_\perp n(v k_\perp) \frac{\theta(A-2k_\perp)}{\sqrt{A-2k_\perp}} \tag{8}$$

with $A=2p_\perp - 2a p_\parallel^2$ and $B=2a$ (the $\theta$ function ensures that the integral is real). In the second term of Eq. (8) we have performed the $k_\parallel$ integration by pushing the momentum cutoff to infinity. The main point is that the former expression can now be integrated by parts to give a further $\Delta$ constraint on $k_\perp$:[9]

$$L = \frac{1}{\sqrt{B}}\int_{-\Lambda}^{A/2} dk_\perp \sqrt{A-2k_\perp}\,\Delta(v k_\perp) + \cdots, \tag{9}$$

where the ellipsis stands for terms that are not confined to the region near the FS. By inspection of the results for $A \gg T/v$, $A \ll -T/v$, and $A \approx 0$, respectively, we see that the $\Delta(v k_\perp)$ function behaves qualitatively as $\delta(v k_\perp + T)$. Therefore, to study the temperature dependence of the susceptibility we can replace the previous expression by

$$L \sim \frac{\sqrt{A/2 + T/v}}{v\sqrt{a}}, \tag{10}$$

where there is an implicit $\theta$ function of the argument of the square root. We are left with a tractable expression for the real part of the Lindhard function, which we shall use to evaluate the two-loop diagram of Fig. 2(a).

We now perform the remaining integrals in Eq. (1) in the following order: $dq_\perp, dp_\perp$, then $dp_\parallel$ and $dq_\parallel$. The first integral is trivial, since $q_\perp$ enters only in $\Delta(\xi_{\mathbf{p}+\mathbf{Q}})$. Moreover, $\xi_{\mathbf{p}+\mathbf{Q}}$ is linear in $q_\perp$ [cf. Eq. (7)] so that the integration just gives $1/v$. The $p_\perp$ integral can also be performed straightforwardly, and we are left with an expression of the form

$$\chi \sim \frac{\tilde{U}^2}{v^3\sqrt{a}} \int dq_\parallel \int dp_\parallel \sqrt{T/v - a p_\parallel^2}$$

$$\sim \frac{\Lambda \tilde{U}^2}{v^3\sqrt{a}} \int dp_\parallel \sqrt{T/v - a p_\parallel^2} \sim \frac{\Lambda \tilde{U}^2}{v^4 a} T, \tag{11}$$

where again we have neglected unimportant multiplicative factors and defined $\tilde{U}=U(\tilde{\mathbf{Q}})$. Within our treatment, we have recovered the result that the spin susceptibility of an isotropic 2D Fermi liquid is intrinsically linear in temperature.[9] For a circular FS, this can be written as

$$\chi(T) = \chi_0 + \chi_1 T. \tag{12}$$

Incidentally, our calculation suggests that the low-temperature correction to the susceptibility is positive, in agreement with Refs. 9 and 16–18.

### B. Anisotropic FS with inflection points

In the vicinity of an inflection point, the dispersion relation can be written as

$$\xi_k/v = k_y - b k_x^3 + g k_x^4, \tag{13}$$

where $b$ and $g$ can be chosen to be positive. A change of variables similar to Eq. (6) of the preceding section leads to

$$L = \frac{-1}{v}\int dk_\perp n(v k_\perp) \int dk_\parallel \frac{1}{A - 2k_\perp + B k_\parallel^2 + C k_\parallel^4} \tag{14}$$

with $A=2p_\perp - 3bq_\parallel p_\parallel^2 - 2g p_\parallel^4$, $B=3bq_\parallel$, and $C=2g$. The $k_\parallel$ integral can be rewritten in the form

$$I = \frac{1}{C^{1/4}(A-2k_\perp)^{3/4}} \int \frac{dx}{1 + \alpha x^2 + x^4} \tag{15}$$

with $\alpha = (B/\sqrt{C})/\sqrt{A-2k_\perp}$. We shall be interested in the region close to the edge ($k_\perp \simeq A/2$), where $\alpha$ is large and positive. We can then drop the quadratic term and perform the integration:

$$I = \frac{1}{[b q_\parallel (A-2k_\perp)]^{1/2}}. \tag{16}$$

This can be integrated by parts in $dk_\perp$ to give

$$L = \frac{1}{\sqrt{b q_\parallel}} \int_{A/2 - b^2 q_\parallel^2/g}^{A/2} dk_\perp \sqrt{A-2k_\perp}\,\Delta(v k_\perp) + \cdots, \tag{17}$$

where the ellipsis stands for a term which is not confined close to the FS (the limits of integration account for the condition $\alpha \gtrsim 1$). Provided that the $\Delta$ function lies entirely inside the domain of integration, i.e.,

$$q_\parallel > q_{min} = \sqrt{\frac{gT}{b^2 v}}, \tag{18}$$

the result takes the form

$$L \sim \frac{\sqrt{A/2+T/v}}{v\sqrt{bq_\parallel}}. \tag{19}$$

The region of phase space we have just identified is the one that gives the leading temperature dependence in the susceptibility. Indeed, for $k_\perp$ outside the range of integration considered above (implying $\alpha \lesssim 1$), the result of the integral (15) is $I \sim (A-2k_\perp)^{-3/4}$ instead of Eq. (16), leading to a weaker (linear) temperature dependence in the final result. The same holds if we consider a negative $q_\parallel$ ($\alpha<0$).

The calculation now follows the same lines as in the previous case. The $q_\perp$ integration yields a factor $1/v$, and the $p_\perp$ integration can be performed by replacing $\Delta(vp_\perp) \sim \delta(p_\perp - T/v)/v$, which gives

$$\chi \sim \tilde{U}^2 \int_{q_{min}}^{\Lambda} dq_\parallel \int_{-\Lambda}^{\Lambda} dp_\parallel \frac{\sqrt{T/v - bq_\parallel p_\parallel^2 - gp_\parallel^4}}{v^3\sqrt{bq_\parallel}}$$

$$\sim \frac{\tilde{U}^2 T}{bv^4} \int_{q_{min}}^{\Lambda} \frac{dq_\parallel}{q_\parallel} = -\frac{\tilde{U}^2}{bv^4} T \ln\left(\frac{gT}{vb^2\Lambda^2}\right). \tag{20}$$

Taking into account the scattering from the regions of the FS far from the inflection points, whose behavior is given by Eq. (12), the susceptibility reads

$$\chi(T) = \chi_0 + \chi_1 T - \chi_1' T \ln T. \tag{21}$$

Once again, the sign of the correction is such that the susceptibility increases with temperature. However, the contribution coming from the other diagram (b) has opposite sign. As a rule of thumb, one can argue that the overall vertex correction is positive if the effective interaction is peaked around $\tilde{\mathbf{Q}}$ and negative otherwise [it vanishes when the momentum dependence of $U(q)$ is flat, since in that case the two diagrams perfectly cancel].

### C. Special inflection points

The previous analysis assumes the existence of a generic inflection point along the Fermi surface. This is a situation that can be achieved, in an anisotropic system, for a finite range of values of the filling or the chemical potential. These points are characterized by the absence of a quadratic term in the expansion of the dispersion relation around the Fermi surface presented in Eq. (13). For certain values of the parameters, however, which require a fine tuning of the filling or the chemical potential, the cubic coefficient $b$ or the quartic one $g$ in Eq. (13) can be zero as well. Two such situations are schematically shown in Fig. 3.

We first consider the case when the cubic term in the dispersion relation parallel to the Fermi surface vanishes ($b=0$), which is realized in the $t-t'$ Hubbard model in a square lattice (see point $G$ in the top panel of Fig. 3), or in simple tight-binding models on the triangular lattice, for instance. The susceptibility becomes more anomalous than in the generic case discussed previously, as can be seen by letting $b \to 0$ in Eq. (20). One has, respectively, $A = 2p_\perp - 3gq_\parallel^2 p_\parallel^2 - 2gp_\parallel^4$ and $B = 3gq_\parallel^2$. The condition $\alpha \gtrsim 1$ now corresponds to $A - 2k_\perp \lesssim gq_\parallel^4$, which modifies the limits of integration in Eq. (17). Repeating the same arguments as before with $q_{min} = (T/gv)^{1/4}$, we obtain

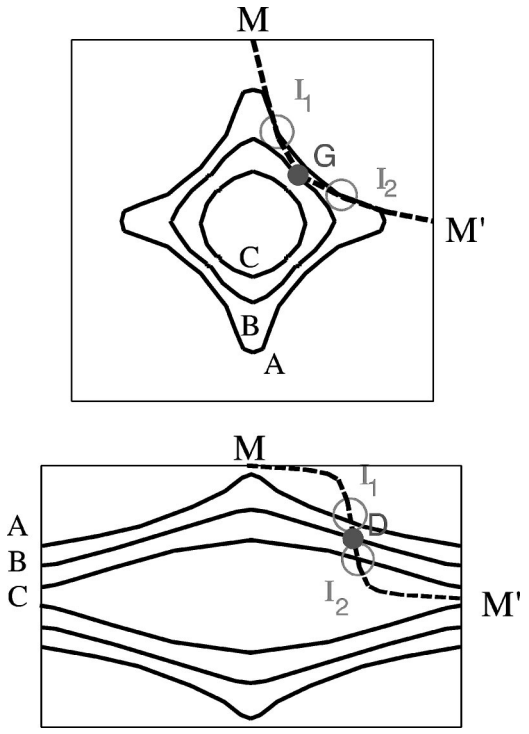


FIG. 3. Top: Fermi surfaces for different fillings in an anisotropic 2D system with tetragonal symmetry. Curve *A* has eight inflection points (only two are shown, $I_1$ and $I_2$). The set of all these points define a curve which goes from point *M* to point $M'$ of the Brillouin zone (broken curve). The inflection points merge in pairs when the Fermi surface is given by curve *B*. At point *G* in curve *B*, the cubic term in the dispersion relation parallel to the Fermi surface vanishes. The Fermi surface labeled *C* has no inflection points. Bottom: Fermi surfaces for different fillings in an anisotropic 2D system with orthorhombic symmetry. Curves *A* and *C* correspond to Fermi surfaces with four inflection points. Only one such point in each curve is shown, $I_1$ and $I_2$. The set of all these points define a curve that goes from point *M* to point $M'$ of the Brillouin zone (broken curve). The quartic term in the dispersion relation parallel to the Fermi surface changes sign when going from *M* to $M'$. Thus, there is a Fermi surface, schematically depicted as curve *B*, where this quartic term vanishes, at point *D*.

$$L = \frac{\sqrt{A/2+T/v}}{v\sqrt{g}q_\parallel} \tag{22}$$

leading to

$$\chi = -\frac{\tilde{U}^2}{v^3}\left(\frac{T}{vg}\right)^{3/4} \ln\left(\frac{T}{gv\Lambda^4}\right). \tag{23}$$

The other possibility is that the quartic term vanishes ($g=0$), which can occur in a tight-binding model with orthorombic symmetry, considering two different hopping parameters $t_a \neq t_b$ (see point *D* in the bottom panel of Fig. 3). In that case, however, not only $g$ but all the even coefficients in the dispersion relation vanish. This leads to perfect nesting

TABLE I. Temperature dependence of the uniform susceptibility of an anisotropic 2D Fermi liquid. The linear contribution is always present, and is due to the portions of the Fermi surface away from the inflection points. The relative magnitude of the regular and anomalous contributions depends on the degree of flatness of the Fermi surface. The special case $b=0$ corresponds to inflection points falling on particular symmetry lines of the Brillouin zone, and requires a fine tuning of the chemical potential (see text).

| Fermi surface geometry | $\chi(T)$ |
|---|---|
| Circular | $\chi_0+\chi_1 T$ |
| Inflection points (generic) | $\chi_0+\chi_1 T-\chi_1' T\ln T$ |
| Special inflection ($b=0$) | $\chi_0+\chi_1 T-\chi_{3/4}T^{3/4}\ln T$ |
| Nesting, saddle points | $\chi_0+\chi_0'\ln T$ |

between opposite branches of the Fermi surface, giving rise to a much more singular behavior $\chi(T)\sim\ln T$.

### D. Self-energy correction

After integration over Matsubara frequencies, which now requires some more attention due to the presence of two fermion lines of equal argument (a double pole in the complex-plane integrals), the anomalous part of the self-energy correction (c) of Fig. 2 can be reduced to the form

$$\chi\sim\tilde{U}^2 T\int d^2Q d^2p d^2k\frac{\Delta(\xi_{\mathbf{k}})\Delta(\xi_{\mathbf{p}})}{(\Delta\xi_{\mathbf{p}}-\Delta\xi_{\mathbf{k}})^2} \qquad (24)$$

with $\Delta\xi_{\mathbf{k}}=\xi_{\mathbf{k}+\mathbf{Q}}-\xi_{\mathbf{k}}$. The $Q$ integration is now restricted to the region close to (within $T/v$ of) $\tilde{\mathbf{Q}}$. We shall not go through all the calculations of the self-energy diagram, which can be performed following the same lines of the previous sections. The results for the temperature dependence are analogous to those given by Eqs. (12), (21) and (23). This can be understood by noting that although the denominator in Eq. (24) is more singular than that of Eq. (3), the additional anomalies that it carries with it are canceled by the explicit $T$ factor in front of Eq. (24), leading to the same temperature dependence as the vertex correction. Its sign is also the same as the vertex diagram (a).

The results of this section are summarized in Table I.

## IV. EXAMPLES

### A. Superconducting cuprates

It is often assumed that a tight-binding model on a square lattice with nearest-neighbor ($t$) and next-nearest-neighbor ($t'$) hopping reproduces well the band structure of the layered cuprates:

$$\varepsilon(\mathbf{k})=-2t(\cos k_x+\cos k_y)-4t'\cos k_x\cos k_y, \qquad (25)$$

where $t'/t\approx-0.25$. This case corresponds roughly to the top set of Fermi surfaces in Fig. 3. The dispersion relation above has a saddle point at a doping $\delta_{VHS}$ corresponding to a chemical potential $E_{VHS}=-4|t'|$. The curvature of the Fermi surface along the diagonals becomes negative at a higher doping $\delta_c$, where the chemical potential is $E_c=-8|t'|+16|t'|^3/t^2$. For fillings such that $E_c\leqslant E_F\leqslant E_{VHS}$, the Fermi surface has eight inflection points. From these values, and the previous analysis, one can obtain a qualitative picture of the temperature dependence of the susceptibilities, when the electron density is in this range.

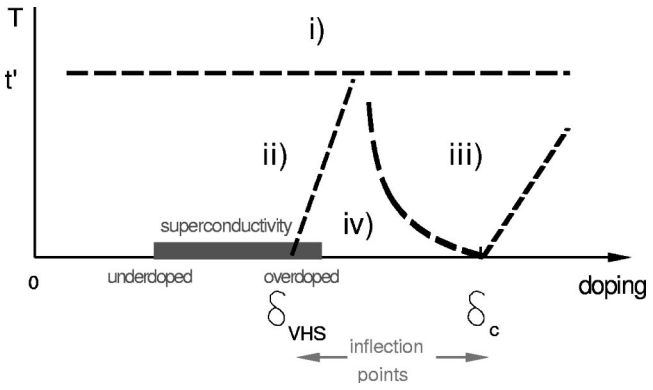


FIG. 4. Correspondence between the different shapes of the Fermi surface discussed in the text and fillings for the high-$T_c$ superconductors.

(i) For $T\gtrsim|t'|$, the susceptibility is determined by $t$ only. As the doping is close to half filling, we expect $\chi(T)\propto|T|^0$, the result for perfect nesting.

(ii) For $T\lesssim|t'|$ and $T\gtrsim|E_F-E_{VHS}|$, the same behavior as in (i) should be observed.

(iii) For $T\lesssim|t'|$ and $T\gtrsim|E_F-E_c|$, the susceptibility is dominated by contribution from the area near the special point discussed in Sec. III C. Hence, $\chi(T)\propto|T|^{3/4}\ln T$.

(iv) For $T\lesssim|t'|$, $T\lesssim|E_F-E_c|$, and $T\lesssim|E_F-E_{VHS}|$, the contributions from the saddle point and from the special point above are absent. Thus, $\chi(T)\propto|T|\ln(T)$, because of the presence of the inflection points.

We can make the estimates of the crossover region in the $T$-doping plane more precise from the doping dependence of the coefficient of the cubic term $b$ in Eq. (13). Expanding around the saddle point, we obtain $b\propto|E_F-E_{VHS}|$. Hence, the crossover between regions (ii) and (iv) takes place at a temperature $T^*\propto|E_F-E_{VHS}|$. Performing a similar calculation around the situation $E_F=E_c$, we have $b\propto\sqrt{|E_F-E_c|}$, so that the crossover temperature is $T^*\propto(E_c-E_F)^2$. For fillings $E_F\sim E_c$ but with no inflection points in the Fermi surface, we obtain a crossover to the $\chi(T)\propto|T|$ behavior due to $2k_F$ scattering, with a crossover temperature $T^*\propto|E_F-E_c|$. The different regimes are schematically shown in Fig. 4.

Taking realistic numbers for the dispersion relation, our analysis predicts anomalous low-temperature behavior in all the region between $\delta_{VHS}$ and $\delta_c$, corresponding to the strongly overdoped region which is experimentally accessible. This shows that nonstandard behavior of the physical properties should be expected even in a regime which is usually believed to be well described by the normal Fermi-liquid theory.

### B. Quasi-1D organic compounds

Organic conductors are often very anisotropic due to the planar structure of their molecules. For example, the salts of

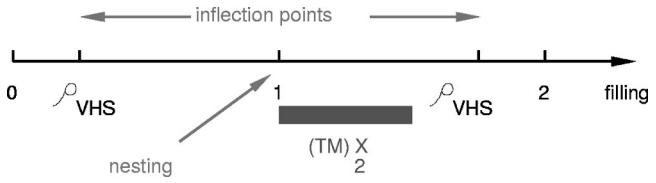


FIG. 5. Correspondence between the different shapes of the Fermi surface discussed in the text and fillings for compounds of the family $(TM)_2X$.

the family $(TM)_2X$ (TM=TMTTF,TMTSF and $X$ =inorganic anion) are all isostructural and can be viewed as two-dimensional arrays of weakly coupled 1D chains, since the electronic overlaps in the transverse direction are 10 times smaller than in the chain direction (the transfer integrals in the third direction are 500 times smaller and can be neglected; see, for instance, Ref. 19). The band structure is well represented as

$$\varepsilon(\mathbf{k}) = -2t_a\cos(k_a a) - 2t_b\cos(k_b b) \tag{26}$$

assuming an orthorombic structure with lattice parameters $b \approx 2a$. This case corresponds to the bottom set of Fermi surfaces in Fig. 3. The parameter $t_b \sim 10$–$30$ meV sets the scale below which the FS is modulated in the $b$ direction, so that the predicted enhancement of susceptibilities due to inflection points should be observable at and below room temperature. The value of the anisotropy ratio $\tau = t_b/t_a$ is large enough to ensure that the system is well described by a Fermi-liquid picture down to very low temperatures. The filling factor $\rho$ is fixed by charge transfer and varies from compound to compound, ranging from 1/2 to 1 hole per TM site. The Fermi surface has two Van Hove singularities at $E_F = \pm E_{VHS} = \pm 2t(1-\tau)$, and four inflection points in the whole interval $0 < |E_F| < E_{VHS}$. Taking $\tau = 0.1$, this corresponds to the region of fillings $0.3 < \rho < 1.7$. In the absence of higher harmonics in Eq. (26), $E_F = 0$ corresponds to half-filling ($\rho = 1$), and the Fermi surface has perfect nesting, as $\varepsilon(\mathbf{k}) = \varepsilon(\mathbf{k}+\mathbf{Q})$, where $\mathbf{Q} = (\pi, \pi)$ (hopping between more distant neighbors will suppress this effect). The points in the phase diagram where the topology of the Fermi surface changes, leading to different behaviors of the electronic susceptibility, are sketched in Fig. 5.

In the $(TM)_2X$ compounds, the spin susceptibility shows a sizable increase in the metallic phase up to room temperature (see, e.g., Fig. 8 of Ref. 19), which cannot be explained by the ''standard'' Fermi-liquid theory (the latter predicts variations on the scale of the Fermi temperature). On the other hand, the presence of enhanced scattering close to inflection points could well be the underlying mechanism of this anomalous temperature dependence, and should be taken into account when studying the low-temperature phase transitions of such compounds.

Following the same procedure used in the preceding section, the electron susceptibility will undergo a succession of crossovers upon varying the filling, which can be achieved either by anion substitution or by applying pressure to the samples.

## V. CONCLUSIONS

We have performed a second-order perturbative calculation to analyze the corrections to the Fermi-liquid behavior in anisotropic interacting electronic systems in two dimensions, which arise from the existence of points in the Fermi surface where scattering is enhanced.[20] Besides the extensively studied case of a saddle point, we have analyzed in detail the influence of inflection points, which do not require any special fine tuning of the chemical potential or the filling. The presence of these points enhances the anomalous dependence on temperature, which arise from $2k_F$ scattering in isotropic Fermi surfaces.[9] We find that the corrections that were linear in $|T|$ change into $|T|\ln|T|$. The absence of symmetries also implies the lack of cancellation between different diagrams, so that these anomalies should be observed in both the spin and charge susceptibilities.

For special fillings, more singular behavior is expected. In the case of systems with tetragonal or hexagonal symmetry, when the Fermi surface is close to these fillings, the corrections to the susceptibilities go as $|T|^{3/4}\ln|T|$, showing that the existence of noninteger $T$ dependences does not need to violate Landau's model for the low-energy excitations of a Fermi liquid.

We have also discussed the possible crossovers between the different regimes analyzed, and the experimental consequences that they may lead to. In the case of the superconducting cuprates, anomalous susceptibilities should appear in the strongly overdoped region, above the doping $\delta_{VHS}$ characterized by Van Hove singularities in the density of states. On the other hand, all of the organic conductors of the family $(TM)_2X$ should fall in the region of fillings where anomalous corrections to the susceptibility are important. Of course, the analysis presented here should also apply to other classes of quasi-two-dimensional systems (heavy-fermion materials, $Sr_2RuO_4$, electrically doped 2D organic films, other organic conductors, etc).

Finally, let us point out that the breakdown of the Sommerfeld expansion for the spin susceptibility suggests that the free energy $\mathcal{F}$ itself has a nonanalytic dependence on $T$, once the high-order interactions ($2k_F$ scattering) are taken into account. If, as was proposed in Refs. 16,21, and 22, and numerically verified in Ref. 23, the role of temperature and magnetic field is interchangeable in the functional form of $\mathcal{F}(T,H)$, one can conclude that the anomalous $T$ dependences calculated here for the susceptibility are also expected in the specific-heat coefficient $\gamma = C/T$.

## ACKNOWLEDGMENTS

We are thankful to R. Markiewicz and M. A. H. Vozmediano for helpful discussions. This work was financially supported by MEC (Spain) through Grant No. PB96-0875, and the European Union through Grant No. FMRXCT980183.

## APPENDIX A: INFLECTION POINTS IN THE $t-t'$ MODEL

We shall determine here the parameters of the dispersion relation (13) in the case of a tight-binding model on a square

lattice with nearest ($t$) and next-nearest ($t'$) neighbor hopping. Let us focus to the doping levels close to $\delta_c$, the point where the inflection points of the Fermi surface merge in pairs on the diagonals of the Brillouin zone, leading to the most singular corrections to the susceptibility. It is then natural to rewrite the dispersion relation in a basis rotated by 45°:

$$\xi = -4t(\cos p \cos q) + 4t'(\cos^2 p - \sin^2 q) - E_F, \quad \text{(A1)}$$

where $p=(k_x+k_y)/2$ and $q=(k_x-k_y)/2$. The Fermi surface crosses the diagonal ($q=0$) at a momentum $p_F$ given by $E_F=-4t\cos p_F+4t'\cos^2 p_F$. The dispersion relation can then be expanded as

$$\xi = A(p-p_F) + Bq^2 + Cq^4 \quad \text{(A2)}$$

with $A=4(t\sin p_F - t'\sin 2p_F)$, $B=2t\cos p_F - 4t'$, and $C=(4/3)[t'-(t/8)\cos p_F]$. The topology of the Fermi surface changes at two well-defined doping levels.

(1) The curvature changes sign at a doping $\delta=\delta_c$ given by the condition $B=0$. The corresponding Fermi energy is $E_c=-8t'+16(t')^3/t^2$ and the coordinates of the inflection point are $(p_c,q_c)=(\arccos 2t'/t,0)$, corresponding to point $G$ of Fig. 3.

(2) Van Hove singularities arise at a doping $\delta_{VHS}$ given by $E_{VHS}=-4t'$ ($M$ points in Fig. 3).

Inflection points appear in all the region of dopings $\delta_{VHS}<\delta<\delta_c$, following the dashed curve of Fig. 3 (top panel). The consequences on the physical properties of the system are summarized in Fig. 4.

*Dispersion around inflection points*. The equation of the Fermi surface is $\xi=0$, which implicitly defines a function $p=p(q)$. Putting the second derivative $p''(q)=0$ yields the coordinates $(p_0,q_0)$ of the inflection points. For $\delta\approx\delta_c$, setting $u=1-4(t'/t)^2$, we can write

$$p_0 = p_c + \frac{E_F-E_c}{4tu^{3/2}}, \quad q_0 = \left(\frac{E_F-E_c}{12ut'}\right)^{1/2} \quad \text{(A3)}$$

so that the trajectory of the inflection points is parabolic around $G$. By expanding around $(p_0,q_0)$, we obtain an equation of the form (13) with

$$v = 4tu^{3/2}, \quad b = \frac{t'}{t}\left(\frac{E_F-E_c}{12t'}\right)^{1/2}, \quad g = \frac{t'}{4tu^{3/2}}. \quad \text{(A4)}$$

## APPENDIX B: INFLECTION POINTS IN THE $t_a-t_b$ MODEL

We shall now derive the parameters of Eq. (13) for a tight-binding model on an orthorombic lattice, with anisotropic hopping ($\tau=t_b/t_a\ll 1$). Let us rewrite for simplicity the dispersion relation (26) as

$$\xi = -2t_a[\cos k + \tau\cos p + \nu] \quad \text{(B1)}$$

with $k=k_a a$, $p=k_b b$, and $\nu=E_F/2t$. The equation of the Fermi surface is $k=\arccos(-\nu-\tau\cos p)$. The number of electrons per site is approximately given by $\rho=2\pi^{-1}\arccos(-\nu)$. The Fermi surface has two Van Hove singularities at $E_{VHS}=\pm 2t(1-\tau)$, and 4 inflection points for any $0<|E_F|<E_{VHS}$. At half-filling ($E_F=0$), the two branches of the open Fermi surface are perfectly nested. The physical consequences of the changes in the Fermi-surface topology occurring at those special fillings are sketched in Fig. 5.

*Dispersion around inflection points*. By setting $k''(p)=0$ we find that the inflection points are located at

$$p_0 = \arccos\left(\frac{\tau\nu}{1-\nu^2}\right), \quad k_0 = \arccos\left(-\nu - \frac{\tau^2\nu}{1-\nu^2}\right). \quad \text{(B2)}$$

For filling levels close to $\nu=0$ (half-filling), the location of the inflection points describes a straight line of slope $-\tau/\sqrt{1-\nu^2}$ in the $(k,p)$ plane (see bottom panel of Fig. 3). After a rotation of the coordinate axes, we obtain an equation of the form (13) with

$$v = 2t\sqrt{1-\nu^2}, \quad b = \frac{\tau}{6\sqrt{1-\nu^2}}, \quad g = -\frac{\nu\tau^2}{24(1-\nu^2)^{3/2}}. \quad \text{(B3)}$$

The approach to the perfect nesting situation at half-filling is signaled by a vanishing $g$, the coefficient of the quartic term in the dispersion relation.

*Permanent address: LEPES/CNRS, BP 166, F-38042 Grenoble Cedex 9, France.


[1] J. Hertz, Phys. Rev. B **14**, 1165 (1976).

[2] T. Moriya, *Spin Fluctuations in Itinerant Electron Magnetism* (Springer, Berlin, 1985).

[3] A.J. Millis, Phys. Rev. B **48**, 7183 (1993).

[4] D. Belitz, T.R. Kirkpatrick, and T. Vojta, Phys. Rev. B **55**, 9452 (1997).

[5] R. Shankar, Rev. Mod. Phys. **66**, 129 (1994).

[6] J. Polchinski, in *Proceedings of the 1992 TASI in Elementary Particle Physics*, edited by J. Harvey and J. Polchinski (World Scientific, Singapore, 1992).

[7] W. Metzner, C. Castellani, and C. Di Castro, Adv. Phys. **47**, 317 (1998).

[8] D. Belitz, T.R. Kirkpatrick, and T. Vojta, Phys. Rev. Lett. **82**, 4707 (1999).

[9] G.Y. Chitov and A.J. Millis, Phys. Rev. Lett. **86**, 5337 (2001); Phys. Rev. B **64**, 054414 (2001).

[10] J. Labbé and J. Bok, Europhys. Lett. **3**, 1225 (1987); J. Friedel, J. Phys. (Paris) **48**, 1787 (1987); **49**, 1435 (1988); H.J. Schulz, Europhys. Lett. **4**, 609 (1987); R.S. Markiewicz and B.G. Giessen, Physica C **160**, 497 (1989); R.S. Markiewicz, J. Phys.: Condens. Matter **2**, 665 (1990); D.M. Newns, H.R. Krishnamurthy, P.C. Pattnaik, C.C. Tsuei, and C.L. Kane, Phys. Rev. Lett. **69**, 1264 (1992).

[11] J. González, F. Guinea, and M.A.H. Vozmediano, Europhys. Lett. **34**, 711 (1996); Nucl. Phys. B **485**, 694 (1997); Phys. Rev. Lett. **84**, 4930 (2000).

[12] J. González, F. Guinea, and M.A.H. Vozmediano, Phys. Rev. Lett. **79**, 3514 (1997); Int. J. Mod. Phys. B **13**, 2545 (1999).

[13] M.H.S. Amin, Ph.D. thesis, University of British Columbia, 1999,

cond-mat/0011455 (unpublished).

[14] This is the finite-temperature generalization, within our perturbative treatment, of the well-known Fermi-Liquid formula expressing the singularity of $G(k)G(k+q)$ lines in the vertex function, see, e.g., A.A. Abrikosov, L.P. Gorkov, and I. E. Dzyaloshinski, *Methods of Quantum Field Theory in Statistical Physics* (Dover, New York, 1975).

[15] The momentum cutoff should, in principle, be different in the $x$ and $y$ directions, but this is of no practical relevance here.

[16] S. Misawa, J. Phys. Soc. Jpn. **68**, 2172 (1999).

[17] S. Misawa, T. Tanaka, and K. Tsuru, Europhys. Lett. **14**, 377 (1991).

[18] D.S. Hirashima and H. Takahashi, J. Phys. Soc. Jpn. **67**, 3816 (1998).

[19] C. Bourbonnais and D. Jérome, in *Advances in Synthetic Metals, Twenty years of Progress in Science and Technology*, edited by P. Bernier, S. Lefrant, and G. Bidan (Elsevier, New York, 1999), pp. 206–301.

[20] We have implicitly assumed that long-range interactions are screened. We have not extended our results to infinite order, which would allow a self-consistent treatment of the screening processes. However, bubble summations, such as those in the random-phase approximation, can be easily carried out using the results presented here. The main feature to be expected is the existence of significant anisotropies in the screened potential.

[21] S. Misawa, Physica B **149**, 162 (1988).

[22] S. Misawa, Physica B **294-295**, 10 (2001).

[23] D.S. Hirashima and K. Kubo, J. Phys. Soc. Jpn. **68**, 2174 (1999).